Volcanic biotite-sanidine $^{40}Ar/^{39}Ar$ age discordances reflect Ar partitioning and pre-eruption closure in biotite

John M. Hora[1,2], Brad S. Singer[1], Brian R. Jicha[1], Brian L. Beard[1], Clark M. Johnson[1], Shan de Silva[3], and Morgan Salisbury[3]

[1]Department of Geoscience, University of Wisconsin, 1215 W. Dayton Street, Madison, Wisconsin 53706, USA
[2]Geowissenschaftliches Zentrum der Universität Göttingen, Abteilung Geochemie, Goldschmidtstraße 1, 37077 Göttingen, Germany
[3]Department of Geosciences, Oregon State University, Corvallis, Oregon 97331-5506, USA

ABSTRACT

The $^{40}Ar/^{39}Ar$ radioisotope system is widely used to date eruption and cooling of volcanic tephra–marker horizons that commonly provide the only means of correlating and assigning numerical ages to stratigraphy in which they are contained. This chronometer bridges the gap between ^{14}C and longer-lived isotopic systems that are too imprecise for dating young samples. However, $^{40}Ar/^{39}Ar$ ages obtained from coevally erupted biotite and sanidine do not always match. Here, we use an independent chronometer, ^{238}U-^{230}Th disequilibrium, to demonstrate that $^{40}Ar/^{39}Ar$ age disparity is not caused by differences in pre-eruption crystallization times. Our findings indicate that the presence of extraneous ^{40}Ar in biotite, and its absence in sanidine, may result from violations of two assumptions implicit in $^{40}Ar/^{39}Ar$ geochronology on volcanic samples: (1) Prior to eruption, minerals are devoid of ^{40}Ar due to rapid loss to an "infinite reservoir" such as the atmosphere, and (2) closure to volume diffusion is geologically instantaneous and coincident with eruption. We propose a mechanism whereby the presence of extraneous Ar in certain minerals is explained by the relative sequence of four events in a magmatic system: (1) crystallization, (2) mineral closure with respect to Ar diffusion, (3) isotopic equilibration of magmatic and atmospheric Ar, and (4) quenching of the system by eruption. These data have potentially far-reaching implications for studies that depend on geochronological data, necessitating re-evaluation of interpretations based solely on biotite with no independent age control, particularly in young samples where the effects are most pronounced.

INTRODUCTION

In the ^{40}K-^{40}Ar system, radiogenic daughter nuclide accumulation begins (i.e., diffusive loss of ^{40}Ar ceases) at temperatures that are relatively low compared to other isotopic systems (e.g., Rb-Sr, Sm-Nd, U-series), thereby recording the cooling of volcanic units. $^{40}Ar/^{39}Ar$ ages have been used in this capacity to calibrate portions of the geologic time scale (Gradstein et al., 2004), correlate stratigraphy (Smith et al., 2006), delineate geomagnetic polarity reversals (Singer et al., 2005), and constrain the pace of hominid evolution and migration (Leakey et al., 1998; Swisher et al., 1994) by providing numerical ages that bracket the geological events of interest. These ages are fundamental to our understanding of the recent geological and climatological evolution of Earth and life on it. Ar geochronology's expanding role in dating Neogene events has largely been driven by analytical advances that allowed increasingly precise $^{40}Ar/^{39}Ar$ measurements to be made on young samples (Chen et al., 1996; Hu et al., 1994; Renne et al., 1997). To avoid flawed interpretations, evaluations of geological reasons behind apparently precise yet inaccurate data are needed, because systematic errors of constant absolute magnitude have increasing relative contribution when applied to younger samples.

Biotite and sanidine are commonly used K-rich mineral phases in K-Ar and $^{40}Ar/^{39}Ar$ dating. Sanidine is a proven chronometer, whereas biotite, despite continued use, is frequently complicated by extraneous ^{40}Ar that manifests as anomalously old ages. Extraneous Ar is present in numerous phases in varied geologic settings (e.g., metamorphic rocks)—and indeed some aspects of the present discussion (i.e., partitioning) may be more broadly applicable—however, here we focus on behavior of Ar in magmatic systems. Biotite and sanidine coexist in dacitic-rhyolitic magmas where this chronometer is commonly used and age discordance is prevalent (e.g., Bachmann et al., 2007; Spell and Harrison, 1993). Whereas previous studies have established that age discordance occurs, the number of independent analyses for a given phase within any single sample has been limited. Consequently, it has been difficult to gauge the magnitude and reproducibility of apparent age differences, or establish whether differences in pre-eruption crystal residence times can account for the discordance. Our goals here are to more thoroughly document biotite $^{40}Ar/^{39}Ar$ age anomalies, independently determine pre-eruption residence times, and offer a conceptual explanation.

$^{40}Ar/^{39}Ar$ GEOCHRONOLOGY

Results

We present the largest currently available database of $^{40}Ar/^{39}Ar$ analyses on coeval volcanic biotite (148 single-crystal total fusions [TF] and 25 incremental heating experiments [IH] using both laser and furnace) and sanidine (251 TF and 53 laser IH) (Table DR1 in the GSA Data Repository[1]). All samples are from rhyolitic and dacitic magmas erupted from the Andean Central Volcanic Zone, range in age from 5.6 Ma to 40 ka, and represent a variety of eruptive styles and volumes (~800 km^3 ignimbrites to 4 km^3 domes): five units from the Altiplano-Puna volcanic complex (APVC) (de Silva, 1989), three units from Cerro Galan, and lava domes associated with Parinacota volcano (Hora et al., 2007). Incremental heating data indicate that sanidine typically yields younger and more precise ages than biotite (Fig. 1A), and biotite age determinations are not in agreement with one another (Fig. 1B). The biotite grains used in our study were large (typically >1 mm diameter, >200 μm thick; Fig. DR1 in the Data Repository), precluding ^{39}Ar recoil-loss as a mechanism (Paine et al., 2006) for anomalously old biotite ages. The crystals are sourced from apparently nonaltered rocks in one of the driest environments on Earth, making parent isotope redistribution by weathering (Roberts et al., 2001) or the presence of intergrown alteration phases (Smith et al., 2008) unlikely causes of the excess age.

Interpretation

Whereas Singer et al. (1998) resolved radiogenic, inherited, and trapped ^{40}Ar components in a heterogeneous mixture of plagioclase phenocrysts and xenocrysts of contrasting age, biotites in general rarely exhibit saddle-shaped spectra (Lanphere and Dalrymple, 1976) associated with excess Ar ($^{40}Ar_{xs}$). More commonly, high-T $^{40}Ar_{xs}$ is substantially homogenized with radiogenic $^{40}Ar^*$ upon analysis (Renne, 1995). This situation is undetectable using the inverse isochron method, explaining why most of our biotite IH yield atmospheric $^{40}Ar/^{36}Ar$ intercepts. Furthermore, biotite, like other hydrous sheet silicates, is unstable during

[1]GSA Data Repository item 2010256, comprising Figures DR1–DR4, Tables DR1–DR5, and Text File DR1, is available online at www.geosociety.org/pubs/ft2010.htm, or on request from editing@geosociety.org or Documents Secretary, GSA, P.O. Box 9140, Boulder, CO 80301, USA.

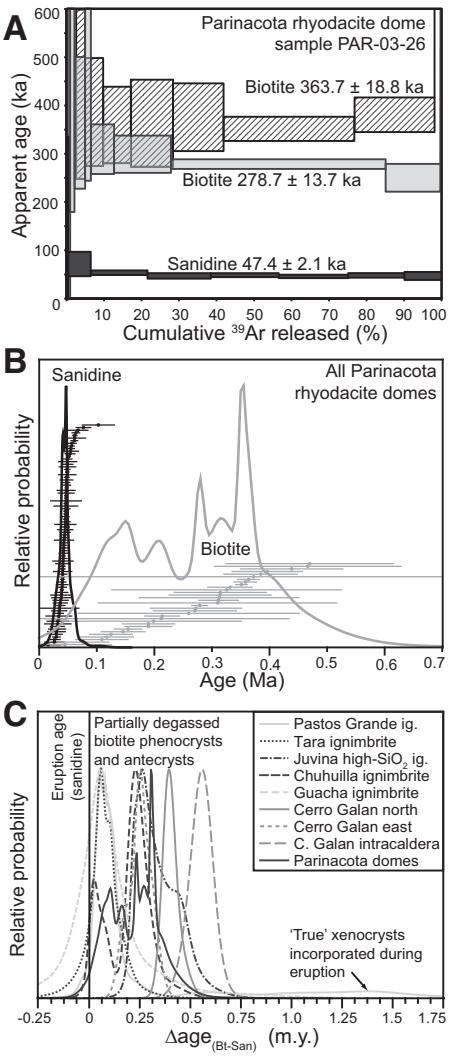

Figure 1. ^{40}Ar/^{39}Ar age discordance. A: Representative biotite and sanidine ^{40}Ar/^{39}Ar age spectra from the same Parinacota rhyodacite dome sample. Despite extreme discordance between analyzed aliquots, all increments of any individual step-heating experiment are concordant. B: Relative probability plot of sanidine (black symbols) and biotite (gray) ^{40}Ar/^{39}Ar apparent ages from Parinacota dome samples. Each dot represents a single incremental heating or total fusion; horizontal lines indicate ±2σ uncertainty; >90% of analyzed sanidine is concordant with the sanidine analysis shown in A, constituting a well-defined probability maximum. Biotites form a broad distribution skewed toward older apparent ages. Stratigraphy constrains dome age to <116 ka and >30 ka, indicating that sanidines provide accurate eruption ages. C: Relative probability distributions for Δage from all studied units, allowing comparison irrespective of eruptive age; biotite ages are consistently older.

vacuum heating, and gas release occurs via dehydration reactions instead of volume diffusion (Harrison et al., 1985; Lo et al., 2000).

Concordance of step ages within a single experiment (Fig. 1A) is therefore not surprising in the context of these problems, and may mask true intracrystal Ar distributions. In this study, we use integrated and total fusion ages, as these are indicative of bulk Ar isotope composition. The magnitude of the age difference between coeval biotite and sanidine (Δage) is limited (<600 k.y.; Fig. 1C), implying an upper limit for the process responsible.

^{238}U-^{230}Th DISEQUILIBRIA

Previously, ^{40}Ar/^{39}Ar age differences were attributed to differing ages of the crystals themselves, i.e., differing pre-eruption residence times (Bachmann et al., 2007) that have been documented in large-volume silicic systems (Charlier and Zellmer, 2000; Reid et al., 1997). There is a paucity of crystal residence time data for small-volume (<10 km^3) silicic systems like those that fed the Parinacota rhyodacite domes, which show similar biotite-sanidine age discrepancies previously observed in large systems. Because of their youth, the Parinacota lava domes present a unique opportunity to both measure the magnitude of biotite age excess and independently determine crystallization ages of the phases involved via ^{238}U-^{230}Th disequilibrium (applicable to samples younger than 300 ka).

^{238}U-^{230}Th data (Table DR2) indicate that both biotite and sanidine predate eruption by up to ~120 k.y. (Fig. 2), but sanidine shows no evidence of this prior history in its ^{40}Ar/^{39}Ar age. This implies substantial differences in partitioning and/or degassing behavior for Ar among sanidine and biotite prior to eruption; consequently a valid model of excess age in biotite must also explain why equally old sanidine crystals are devoid of extraneous ^{40}Ar.

PARTITIONING

Because most biotite ^{40}Ar/^{39}Ar ages are older than the sum of independently known eruption age and pre-eruption crystal residence time constrained by ^{238}U-^{230}Th disequilibria, in situ–produced inherited Ar (^{40}Ar$_K$) cannot be the sole reason for discordance; externally sourced ^{40}Ar$_{xs}$ must also be present. Noble gasses are normally thought to be very incompatible in minerals and melts (Kelley, 2002). Transit of Ar through a magmatic system is commonly viewed as unidirectional: (1) sourced in K-rich minerals, (2) followed by rapid diffusion into the surrounding melt, which approximates a zero-concentration boundary (Baxter et al., 2002), and (3) degassing to its ultimate sink, the atmosphere. This model is valid at low pressures during and after eruption and implies that Ar concentrations in minerals and the melt are low. Elevated partial pressure of Ar (p_{Ar}) invalidates the zero-concentration boundary approximation, and equilibrium concentrations of Ar in minerals are dictated by their relative solubilities: vapor phase >> melt >> biotite > sanidine (Kelley, 2002), all

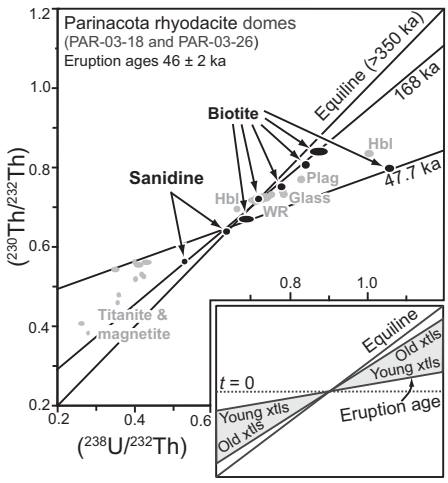

Figure 2. Parinacota dome ^{238}U-^{230}Th crystallization ages. On an equiline diagram, a short-lived burst of crystallization produces a linear isochron. Protracted crystallization (cf. Charlier and Zellmer, 2000) produces wedges bounded by isochrons indicating onset and cessation of crystallization (inset). Parinacota dome minerals span ~120 k.y. bounded by isochrons of 168 and 47.7 ka; the younger isochron is in close agreement with sanidine-determined ^{40}Ar/^{39}Ar eruption ages (46 ± 2 ka). Ellipses indicate 2σ external reproducibility. WR—whole rock; Plag—plagioclase; Hbl—hornblende. The relative position of any given phase within the wedge gives an approximation of its (bulk) age—long-lived crystals have cores that are older and rim ages that are younger than this "integrated" age. With one exception, both sanidine and biotite are ~120 k.y. older than eruption, as they plot near the older bounding isochron.

of which are proportional to p_{Ar} (Table DR3). Solubility in melt increases from basalt to rhyolite by approximately an order of magnitude (Carroll and Stolper, 1993), from <0.1 to 0.8 ppm/bar$_{Ar}$. Therefore, the capacity of melts to act as Ar transfer media between mineral sources and the atmospheric sink decreases with increasing SiO_2 content and pressure.

Because Ar solubility (S_{Ar}) is proportional to p_{Ar}, the maximum amount of ^{40}Ar$_{xs}$, and consequently the predicted maximum age excess (t_{xs}), would, at equilibrium without chemical potential gradients caused by active degassing, depend on total pressure (P_{total}), proportion of Ar in the ambient fluid/vapor phase (X_{Ar}), and its (steady-state) isotopic composition (^{40}Ar/^{36}Ar) as

$$t_{xs,Bt} = \frac{1}{\lambda}\ln\left(1+\frac{\lambda}{\lambda_e+\lambda'_e}\cdot\frac{P_{total}X_{Ar}S_{Ar,Bt}}{\left[{}^{40}\mathrm{K}\right]_{Bt}}\cdot\frac{\left({}^{40}\mathrm{Ar}/{}^{36}\mathrm{Ar}\right)-295.5}{\left({}^{40}\mathrm{Ar}/{}^{36}\mathrm{Ar}\right)+1}\right). \quad (1)$$

Equation 1 derivation and values of decay constants (λ) are given in the Data Repository.

Incorporation of atmospheric ^{40}Ar (i.e., $^{40}Ar/^{36}Ar$ = 295.5) does not result in excess age, because this component is subtracted during data processing. At magma storage depths, the impact of high p_{Ar} on age may be twofold: More Ar is partitioned into the minerals, and likelihood of complete atmospheric equilibration is decreased. Observed biotite age excesses require only modest pressures (1–3 km depth), with X_{Ar} approximately two times atmospheric concentrations (~2% of fluid phase), and can occur in magmas that have been substantially (though not completely) equilibrated with the atmosphere (~98% atmospheric Ar, 2% $^{40}Ar_{xs}$; Table DR4).

If preserved, partitioned Ar in minerals would be present in all minerals, according to relative solubilities. Predicted age excess would be approximately 3.8 times smaller in sanidine than in biotite due to lower solubility and higher stoichiometric K content. Because no age excesses are observed in sanidine, any mechanism that explains Δage must lock in $^{40}Ar_{xs}$ in biotite, while allowing it to escape from sanidine once the system becomes open to the atmosphere and reaches the low pressures of eruption.

CLOSURE TEMPERATURE

As the system departs from equilibrium, the proportion of maximum partitioned $^{40}Ar_{xs}$ that is retained in biotite is dictated by kinetics and depends on the shifting balance between net partial loss and net partial retention of Ar (Fig. DR2). At high T, loss depends largely on the chemical potential difference of Ar between crystal and melt (i.e., degree of melt degassing), because diffusion is fast relative to radiogenic ingrowth. Alternating episodes of volatile degassing and recharge <1 yr prior to eruption are recorded by $^{40}Ar_{xs}$ in Mount St. Helens plagioclase (Layer and Gardner, 2001) and by hydroxyl zoning in apatite from Cerro Galan (Boyce and Hervig, 2008). Although H_2O is approximately one order of magnitude more soluble in silicate melts relative to CO_2 and Ar (Carroll and Stolper, 1993), the late loss of volatiles that is implied by apatite zoning (Boyce and Hervig, 2008) suggests that elevated p_{Ar} may persist until shortly prior to eruption.

As the magma cools, the temperature-dependent rate of diffusion determines the transition between loss and retention regimes. Closure temperature (T_c) is a function of phase-specific parameters that describe diffusivity, the size and shape of the diffusion domain, and cooling rate (dT/dt) (Dodson, 1973). Due to large differences in dT/dt found in nature, widely reported "plutonic" T_c are inappropriate for pre-eruption conditions of most volcanic systems, which accumulate, cool, and erupt on shorter time scales. In Figure 3A, we show the dependence of T_c on dT/dt (full results, including dependence on diffusion domain size, in Fig. DR3). For faster pre-eruption dT/dt, amphibole and biotite can partially close to diffusion at higher temperatures, similar to pre-eruption storage for rhyolites, whereas sanidine remains open, even at extremely fast cooling rates (Fig. 3A). We consider post-eruption cooling of a lava or tephra as geologically instantaneous, and only pre-eruption dT/dt enters into the determination of T_c. Determination of the time and ^{40}Ar concentration at which the transition from partial loss to retention occurs is constrained by boundary conditions on degassing rate and timing, $T(t)$, and starting conditions in equation 1 (Fig. DR2). Regardless of the model used, retention of extraneous Ar in biotite, in contrast to the apparently efficient degassing of Ar in sanidine, implies that the relative order of four events is important in determining whether any phase (i.e., biotite and potentially hornblende) yields anomalously old ages: (1) crystallization, (2) closure with respect to volume diffusion, (3) degassing and equilibration with atmospheric Ar, and (4) quenching of the system by eruption (Fig. 3B). If the order of events changes, no age excess will be recorded by the mineral.

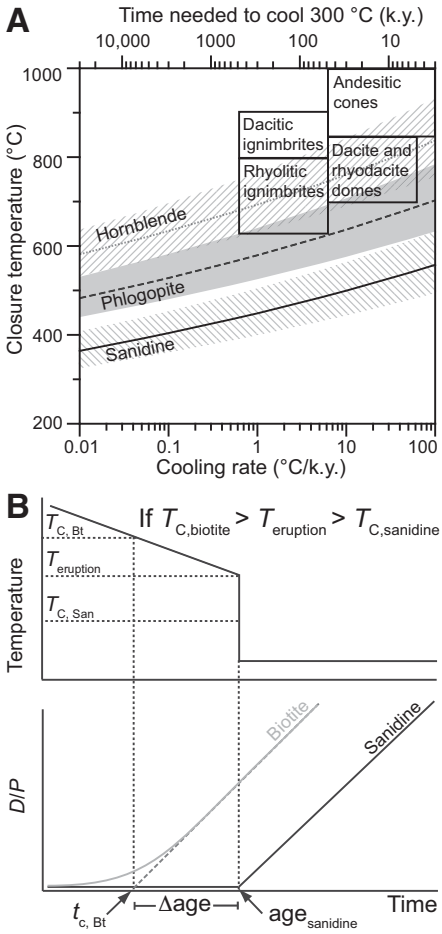

Figure 3. Pre-eruption closure: a mechanism for retention of partitioned $^{40}Ar_{xs}$. A: Closure temperature (T_c) as a function of cooling rate (dT/dt); shaded bands approximate mineral closure intervals—i.e., the range of diffusivities between 10 × D_{Tc} and 0.1 × D_{Tc}. Scale spans the range of crustal storage conditions. Boxes indicate estimated pre-eruption T and dT/dt for volcanic samples. B: Schematic time series in a model system where $T_{c,biotite} > T_{eruption} > T_{c,sanidine}$, shown for the end-member case of inherited $^{40}Ar_K$ only—no $^{40}Ar_{xs}$. As pre-eruption cooling at depth proceeds, biotite passes through its closure interval, initiating gradual increase in daughter nuclide retention (increase in daughter/parent ratio [D/P] analogous to the case of a cooling pluton) before eruption. Its effective time of closure (t_c) reflects early retention. Eruption abruptly decreases temperature. Sanidine passes through its closure interval equally abruptly, and is fully retentive of Ar shortly after eruption (the usual assumption in $^{40}Ar/^{39}Ar$ geochronology on volcanic rocks). With additional partitioned $^{40}Ar_{xs}$, biotite has initial D/P > 0, and Δage will be larger relative to the inheritance-only case (see also Fig. DR2 [see footnote 1]).

Thermometry from several ignimbrites from the Altiplano-Puna volcanic complex indicates storage and eruption at $T \approx T_{c,biotite}$ (Lindsay et al., 2001). For Parinacota domes, Fe-Ti oxide thermometry yields T = 792 ± 30 °C (Table DR5; Fig. DR4). If biotite and hornblende are closed or partially closed prior to eruption, some of the in situ–produced $^{40}Ar_K$ and partitioned $^{40}Ar_{xs}$ may be "locked" in those phases; in contrast, sanidine begins accumulating ^{40}Ar only after coincident eruption and closure (Fig. 3B). Because volcanic groundmass and glass are liquid at the time of eruption, these components behave similarly to sanidine in terms of rapid diffusive equilibration with the atmosphere and likewise give reliable eruption ages, although they are more susceptible to post-eruption alteration (hydration in particular) than sanidine.

DISCUSSION

The magnitude of Δage appears to be determined by the degree of isotopic equilibration with the atmosphere before biotite closure, and whether eruption temperature is lower than biotite T_c. Consequently, extraneous ^{40}Ar contents of 10^{-13} to 10^{-11} mol per gram of biotite limit age excess to <600 k.y. (Fig. 4). Here we show that the discrepancy is not analytical; rather, instrumental precision has approached the level where relatively small systematic differences are detected among phases that compose magma. These data underscore the reliability of sanidine and glass analyses, but they should not be taken as a blanket indictment of $^{40}Ar/^{39}Ar$ geochronology on biotite; adverse effects may be undetectable in samples older than Cretaceous age, or where $T_{eruption} > T_{c,biotite}$. Rather, we urge caution and point to an instance where advances in analytical precision are outpacing our understanding of processes that are recorded in biotite and sanidine respectively. As techniques improve,

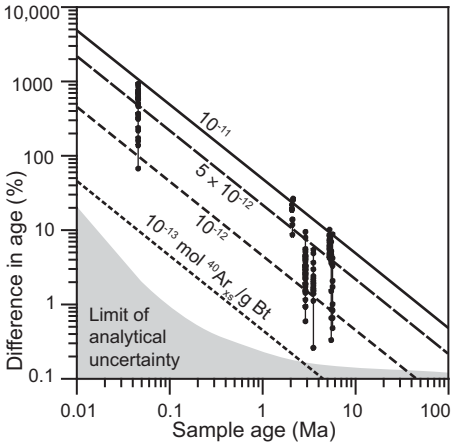

Figure 4. Age discrepancy (%) as a function of sample age. Dots indicate variability of biotite ages for studied units (vertical axis), connected by vertical lines representing corresponding sanidine age (in Ma, horizontal axis). Labeled dashed lines represent equal concentrations of excess Ar, and indicate limits on amount of retained $^{40}Ar_{xs}$ detected in these samples. Gray shaded region represents current limits on analytical precision.

the region beyond analytical limits in Figure 4 will contract, and evaluation of inherent geological limitations on accuracy will be increasingly important. Our findings indicate that sanidine, in general, appears to behave as the common assumptions suggest. Conversely, biotites may retain evidence of pre-eruption conditions that complicate interpretations of their apparent ages.

ACKNOWLEDGMENTS

We thank the Oregon State University Radiation Center for sample irradiation, Sue Kay for supplying Cerro Galan samples, and John Fournelle for assistance with Fe-Ti oxide thermometry. This work was supported by National Science Foundation grant EAR-0538159 to Singer; grants EAR-0538206 and EAR-0710545 to de Silva; and Geological Society of America, Sigma Xi, and Weeks grants to Hora. We thank editor William Collins, Paul Renne, and an anonymous reviewer for comments that improved this manuscript.

REFERENCES CITED

Bachmann, O., Oberli, F., Dungan, M.A., Meier, M., Mundil, R., and Fischer, H., 2007, $^{40}Ar/^{39}Ar$ and U-Pb dating of the Fish Canyon magmatic system, San Juan Volcanic field, Colorado: Evidence for an extended crystallization history: Chemical Geology, v. 236, p. 134–166, doi: 10.1016/j.chemgeo.2006.09.005.

Baxter, E.F., DePaolo, D.J., and Renne, P.R., 2002, Spatially correlated anomalous $^{40}Ar/^{39}Ar$ "age" variations in biotites about a lithologic contact near Simplon Pass, Switzerland: A mechanistic explanation for excess Ar: Geochimica et Cosmochimica Acta, v. 66, p. 1067–1083, doi: 10.1016/S0016-7037(01)00828-6.

Boyce, J.W., and Hervig, R.L., 2008, Magmatic degassing histories from apatite volatile stratigraphy: Geology, v. 36, p. 63–66, doi: 10.1130/G24184A.1.

Carroll, M.R., and Stolper, E.M., 1993, Noble gas solubilities in melts and glasses: New experimental results for argon and the relationship between solubility and ionic porosity: Geochimica et Cosmochimica Acta, v. 57, p. 5039–5051, doi: 10.1016/0016-7037(93)90606-W.

Charlier, B., and Zellmer, G., 2000, Some remarks on U-Th mineral ages from igneous rocks with prolonged crystallisation histories: Earth and Planetary Science Letters, v. 183, p. 457–469, doi: 10.1016/S0012-821X(00)00298-3.

Chen, Y.S., Smith, P.E., Evensen, N.M., York, D., and Lajoie, K.R., 1996, The edge of time: Dating young volcanic ash layers with the ^{40}Ar-^{39}Ar laser probe: Science, v. 274, p. 1176–1178, doi: 10.1126/science.274.5290.1176.

de Silva, S., 1989, Geochronology and stratigraphy of the ignimbrites from the 21°30′S to 23°30′S portion of the Central Andes of northern Chile: Journal of Volcanology and Geothermal Research, v. 37, p. 93–191, doi: 10.1016/0377-0273(89)90065-6.

Dodson, M.H., 1973, Closure temperature in cooling geochronological and petrological systems: Contributions to Mineralogy and Petrology, v. 40, p. 259–274, doi: 10.1007/BF00373790.

Gradstein, F.M., Ogg, J.G., and Smith, A.G., 2004, A geologic time scale 2004: Cambridge, UK, New York, Cambridge University Press, 589 p.

Harrison, T.M., Duncan, I., and Mcdougall, I., 1985, Diffusion of ^{40}Ar in biotite: Temperature, pressure and compositional effects: Geochimica et Cosmochimica Acta, v. 49, p. 2461–2468, doi: 10.1016/0016-7037(85)90246-7.

Hora, J.M., Singer, B.S., and Wörner, G., 2007, Volcano evolution and eruptive flux on the thick crust of the Andean Central Volcanic Zone: $^{40}Ar/^{39}Ar$ constraints from Volcán Parinacota, Chile: Geological Society of America Bulletin, v. 119, p. 343–362, doi: 10.1130/B25954.1.

Hu, Q., Smith, P.E., Evensen, N.M., and York, D., 1994, Lasing in the Holocene: Extending the ^{40}Ar-^{39}Ar laser probe method into the ^{14}C age range: Earth and Planetary Science Letters, v. 123, p. 331–336, doi: 10.1016/0012-821X(94)90277-1.

Kelley, S., 2002, Excess argon in K-Ar and Ar-Ar geochronology: Chemical Geology, v. 188, p. 1–22, doi: 10.1016/S0009-2541(02)00064-5.

Lanphere, M.A., and Dalrymple, G.B., 1976, Identification of excess ^{40}Ar by $^{40}Ar/^{39}Ar$ age spectrum technique: Earth and Planetary Science Letters, v. 32, p. 141–148, doi: 10.1016/0012-821X(76)90052-2.

Layer, P.W., and Gardner, J.E., 2001, Excess argon in Mount St. Helens plagioclase as a recorder of magmatic processes: Geophysical Research Letters, v. 28, p. 4279–4282, doi: 10.1029/2001GL013855.

Leakey, M.G., Feibel, C.S., McDougall, I., Ward, C., and Walker, A., 1998, New specimens and confirmation of an early age for *Australopithecus anamensis*: Nature, v. 393, p. 62–66, doi: 10.1038/29972.

Lindsay, J.M., Schmitt, A.K., Trumbull, R.B., de Silva, S.L., Siebel, W., and Emmermann, R., 2001, Magmatic evolution of the La Pacana caldera system, Central Andes, Chile: Compositional variation of two cogenetic, large-volume felsic ignimbrites: Journal of Petrology, v. 42, p. 459–486, doi: 10.1093/petrology/42.3.459.

Lo, C.H., Lee, J.K.W., and Onstott, T.C., 2000, Argon release mechanisms of biotite in vacuo and the role of short-circuit diffusion and recoil: Chemical Geology, v. 165, p. 135–166, doi: 10.1016/S0009-2541(99)00167-9.

Paine, J.H., Nomade, S., and Renne, P.R., 2006, Quantification of ^{39}Ar recoil ejection from GA1550 biotite during neutron irradiation as a function of grain dimensions: Geochimica et Cosmochimica Acta, v. 70, p. 1507–1517, doi: 10.1016/j.gca.2005.11.012.

Reid, M.R., Coath, C.D., Harrison, T.M., and McKeegan, K.D., 1997, Prolonged residence times for the youngest rhyolites associated with Long Valley Caldera: ^{230}Th-^{238}U ion microprobe dating of young zircons: Earth and Planetary Science Letters, v. 150, p. 27–39, doi: 10.1016/S0012-821X(97)00077-0.

Renne, P.R., 1995, Excess ^{40}Ar in biotite and hornblende from the Noril'sk 1 intrusion, Siberia: Implications for the age of the Siberian Traps: Earth and Planetary Science Letters, v. 131, p. 165–176, doi: 10.1016/0012-821X(95)00015-5.

Renne, P.R., Sharp, W.D., Deino, A.L., Orsi, G., and Civetta, L., 1997, $^{40}Ar/^{39}Ar$ dating into the historical realm: Calibration against Pliny the Younger: Science, v. 277, p. 1279–1280, doi: 10.1126/science.277.5330.1279.

Roberts, H.J., Kelley, S.P., and Dahl, P.S., 2001, Obtaining geologically meaningful ^{40}Ar-^{39}Ar ages from altered biotite: Chemical Geology, v. 172, p. 277–290, doi: 10.1016/S0009-2541(00)00255-2.

Singer, B.S., Wijbrans, J.R., Nelson, S.T., Pringle, M.S., Feeley, T.C., and Dungan, M.A., 1998, Inherited argon in a Pleistocene andesite lava: $^{40}Ar/^{39}Ar$ incremental-heating and laser-fusion analyses of plagioclase: Geology, v. 26, p. 427–430, doi: 10.1130/0091-7613(1998)026<0427:IAIAPA>2.3.CO;2.

Singer, B.S., Hoffman, K.A., Coe, R.S., Brown, L.L., Jicha, B.R., Pringle, M.S., and Chauvin, A., 2005, Structural and temporal requirements for geomagnetic field reversal deduced from lava flows: Nature, v. 434, p. 633–636, doi: 10.1038/nature03431.

Smith, M.E., Singer, B.S., Carroll, A.R., and Fournelle, J.H., 2006, High-resolution calibration of Eocene strata: $^{40}Ar/^{39}Ar$ geochronology of biotite in the Green River Formation: Geology, v. 34, p. 393–396, doi: 10.1130/G22265.1.

Smith, M.E., Singer, B.S., Carroll, A.R., and Fournelle, J.H., 2008, Precise dating of biotite in distal volcanic ash: Isolating subtle alteration using $^{40}Ar/^{39}Ar$ laser incremental heating and electron microprobe techniques: American Mineralogist, v. 93, p. 784–795, doi: 10.2138/am.2008.2517.

Spell, T.L., and Harrison, T.M., 1993, $^{40}Ar/^{39}Ar$ geochronology of post-Valles Caldera rhyolites, Jemez Volcanic Field, New Mexico: Journal of Geophysical Research (Solid Earth), v. 98, p. 8031–8051, doi: 10.1029/92JB01786.

Swisher, C.C., Curtis, G.H., Jacob, T., Getty, A.G., and Suprijo, A., 1994, Age of the earliest known hominids in Java, Indonesia: Science, v. 263, p. 1118–1121, doi: 10.1126/science.8108729.

Manuscript received 27 January 2010
Revised manuscript received 18 May 2010
Manuscript accepted 21 May 2010

Printed in USA

Geology

Volcanic biotite-sanidine $^{40}Ar/^{39}Ar$ age discordances reflect Ar partitioning and pre-eruption closure in biotite

John M. Hora, Brad S. Singer, Brian R. Jicha, Brian L. Beard, Clark M. Johnson, Shan de Silva and Morgan Salisbury

Geology 2010;38;923-926
doi: 10.1130/G31064.1

Notes